

Oscillations in SIRS model with distributed delays

Sebastián Gonçalves¹, G. Abramson² and Marcelo F. C. Gomes¹

¹Instituto de Física, Universidade Federal do Rio Grande do Sul, Caixa Postal 15051, 90501-970 Porto Alegre RS, Brazil

²Centro Atómico Bariloche, CONICET and Instituto Balseiro, 8400 S. C. de Bariloche, Argentina

E-mail: sgonc@if.ufrgs.br

E-mail: abramson@cab.cnea.gov.ar

E-mail: marfcg@if.ufrgs.br

Abstract. The ubiquity of oscillations in epidemics presents a long standing challenge for the formulation of epidemic models. Whether they are external and seasonally driven, or arise from the intrinsic dynamics is an open problem. It is known that fixed time delays destabilize the steady state solution of the standard SIRS model, giving rise to stable oscillations for certain parameters values. In this contribution, starting from the classical SIRS model, we make a general treatment of the recovery and loss of immunity terms. We present oscillation diagrams (amplitude and period) in terms of the parameters of the model, showing how oscillations can be destabilized by the shape of the distributions of the two characteristic (infectious and immune) times. The formulation is made in terms of delay equation which are both numerical integrated and linearized. Results from simulation are included showing where they support the linear analysis and explaining why not where they do not. Considerations and comparison with real diseases are presented along.

PACS numbers: 87.19.X-, 87.23.Cc

1. Introduction

Many diseases that have affected and still affect humans come and go with time in a well established way. Examples are plenty and fill the bulletins of world and national health organizations. Measles, typhus and cholera epidemic waves, just to cite a few, are even part of mathematical biology books [1, 2]. The common denominator of such diseases is the cyclic natural history of them, in which a susceptible subject can go to infected, then to removed, and finally back to the susceptible state. However, the mere cyclic nature of the disease does not grant an oscillatory behavior of its epidemic, as can be exemplified by gonorrhoea [3, 4]. In 2009 a new variant of influenza A H1N1, dubbed *swine flu*, appeared in the scene taking the media to discuss on the wave behavior of influenza. In which way do these oscillations arise in a population, apparently synchronizing the infective state of many individuals? Are they related to external driving causes, such as the seasons? Or do they arise dynamically from the very natural history of the disease? It is known that several causes can produce oscillations in model epidemic systems: seasonal driving [5], stochastic dynamics [6, 7], a complex network of contacts [8], etc.

In every infectious disease several characteristic times clearly appear in the dynamics. In a SIRS type disease (see figure 1) one has an infectious time (during which the agent stays in category I , infected and infectious), and an immune time (during which the agent stays in category R , recovered from infection, and immune to re-infection until it returns to the susceptible class S). A standard SIRS model uses the inverse of these characteristic times as rates in mass-action equations, showing damped oscillations toward the endemic state in most typical situations. However, the standard SIRS model does not exhibit sustained oscillations for any value of the parameters. Would it be possible for a deterministic SIRS model to sustain oscillations, and if so how do the characteristic times relate to the period of the epidemic? These are some of the questions we address in this contribution.

As observed by Anderson and May [1] the mathematically convenient treatment of the duration of the infection as a constant rate is rarely realistic. It is more common that recovery from infection takes place after some rather well defined time. It would seem a valid simplification to assume that recovery happens *exactly* at a given time, instead of continuously at some rate. Both extremes are called Type B and Type A recovery respectively by Anderson and May. Most infections belong to an intermediate type between these two extremes (but closer to Type B). These intermediate types have an infectious time distributed with a shape between that of an exponential (Type A) and that of a delta distribution (Type B). An accurate model should implement the distributions based on empirical data. And as suggested by Hoppenstaedt and others [9], that could be done replacing the simple constant rate term by an integral, leading to integro-differential equations. Similar considerations can be made about the transition from recovered to susceptible term. It is almost thirty years ago that Hethcote *et al* [10] showed precisely that the SIRS model with fixed delay in the recovered to susceptible transition presents stable periodic solution for certain parameter values. On the other side they demonstrated that fixed delay in the recovery from infection term does not have the same effect when the other one is considered in the usual way. This implies that the immunity time plays the most important role in the emerging oscillations as we will show in detail. Recently, continuing with the work of Hethcote *et al*, Taylor and Carr [11] studied in detail the dynamics of the SIRS model with temporary immunity, but considering that a fraction of the population acquire permanent immunity. In other words, that is equivalent to a distribution of immunity times made of two delta peaks (at a finite time and at infinite). That makes the analysis of the oscillations much more involved because of the extra parameter: the fraction of individuals who became permanently removed.

Our contribution can be regarded as an extension of the work of Hethcote *et al* with time delays, in which we use arbitrary distributions of both infectious and immune times. While doing this we want to keep the problem as simple as possible in terms of parameters, thus we avoid the use of vital dynamics. We start by considering the most extreme case: fixed delay in both terms (delta distributions). This is the simplest mathematical case in terms of delays, and it is close related with the first case studied by Hethcote *et al*. [10]. Then, we consider a mono-parametric family of models in which the times are described by continuous distributions —being possible to go continuously from a Type B to a Type A model for example. In other words we go from the SIRS model with deterministic delays to the classical constant rates SIRS, taking all the intermediate situations in between. In this way, while we cover previous results, we can go further considering the most general situation for a SIRS model.

For delayed models, we analyze the onset of sustained oscillations and characterize them with the parameters of the system. Linear analysis, together with numerical solutions of the nonlinear model, provide a clear characterization of the phenomenon. Stochastic numerical simulations provide further support to our analysis. Moreover, we show the effect of the shape of the distributed delays on the stabilization of the

oscillations. Besides, the oscillations period, which may play an important role in the design of intervention policies, are shown to satisfy general rules in terms of the SIRS parameters.

2. SIRS model with arbitrary recovery and loss of immunity dynamics

As mentioned above, the usual formulation of a SIRS model implies that recovery from infection, $I \rightarrow R$, proceeds at a rate which is independent of the moment of infection. Also, the loss of immunity $R \rightarrow S$ is also just proportional to the current sub-population and proceeds at its own rate. The mathematical formulation of such a model is usually presented in terms of differential equations as follows:

$$\frac{ds(t)}{dt} = -\beta s(t) i(t) + \frac{r(t)}{\tau_r}, \quad (1a)$$

$$\frac{di(t)}{dt} = \beta s(t) i(t) - \frac{i(t)}{\tau_i}, \quad (1b)$$

$$\frac{dr(t)}{dt} = \frac{i(t)}{\tau_i} - \frac{r(t)}{\tau_r}, \quad (1c)$$

where $s(t)$, $i(t)$ and $r(t)$ stand for the corresponding fractions of susceptible, infectious and recovered individuals in the population ($s(t) + i(t) + r(t) = 1$). The parameters of the model are β , the contagion rate per individual, and τ_i and τ_r , the characteristic infectious and immunity periods respectively[‡]

The analysis of more general systems—in which the recovery from infection and loss of immunity processes obey more general and more realistic dynamics—is more involved, leading to non-local integro-differential equations. Before proceeding to the most general situation, we analyze the simplest case of *fixed times*.

2.1. SIRS with fixed infectious and immunity times

Let us assume that the disease is characterized by an *infectious time* τ_i as well as an *immunity time* τ_r . That is, an individual that becomes infectious at time t will *deterministically* recover at time $t + \tau_i$, becoming immune, and will subsequently lose its immunity at time $t + \tau_i + \tau_r \equiv t + \tau_0$, becoming susceptible again. The process is schematically depicted in figure 1. This system can be represented by the following set

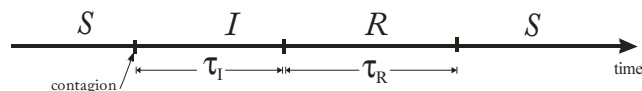


Figure 1. Timeline of an individual, showing the course of the disease after contagion.

[‡] Note on nomenclature: the *infectious* time is frequently called as *recovery* time as well, because it marks the passage from I to R which is the recovery from infection. While we prefer the first name, in order to avoid ambiguities with labels we associate them to the classes, i.e.: τ_i is the time in the infective class, τ_r is the time in the recovered class.

of equations for the fraction of susceptible and infectious sub-populations (bear in mind that $r(t) = 1 - s(t) - i(t)$, so that just two equations describe the dynamics):

$$\frac{ds(t)}{dt} = -\beta s(t) i(t) + \beta s(t - \tau_0) i(t - \tau_0), \quad (2a)$$

$$\frac{di(t)}{dt} = \beta s(t) i(t) - \beta s(t - \tau_i) i(t - \tau_i). \quad (2b)$$

Before proceeding with the detailed analysis of the above formulation of the SIRS model we show in figure 2 a result in advance, comparing the time evolution of the fraction of infectives in the two scenarios: the SIRS with two fixed time delays and the standard SIRS. The last one produce the well know behavior of damped oscillations toward the endemic state. Using the same parameters ($\beta = 0.4, \tau_i = 5, \tau_r = 50$) the SIRS with two delays shows clearly the sustained peaked oscillation in the infective fraction. The time delay in the removed to susceptible transition instead of the usual continuous rate transition is the responsible for the oscillation as we will see in the next sections. In general, delay equations applied to SIR like models have noticeable effects on the dynamics, that is different forms of the infection time distribution yield different dynamics for the infectives and susceptibles [12]. The example of figure 2 is a remarkable case.

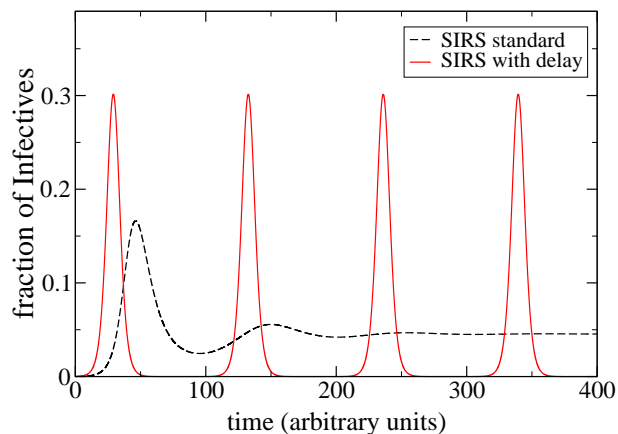


Figure 2. Time evolution of the fraction of infected individuals for the SIRS model. Comparison between the numerical solutions for the standard and the two fixed time delays formulation. Parameters are $\beta = 0.4, \tau_i = 5, \tau_r = 50$.

In equations (2a-2b), the first terms represents the contagion of susceptible by infectious ones, which occurs locally in time at a rate β . The second terms account for loss of infectivity (2b) and loss of immunity (2a). Both terms correspond to the individuals infected at some earlier time: $t - \tau_i$ and $t - \tau_0$ respectively, and who have proceeded through the corresponding stage of the disease. These equations must be supplemented with initial conditions, appropriate for interesting epidemiological situations. A reasonable choice, which we use in the remaining of the paper, is an introduction of infectious subjects into a completely susceptible population:

$$s(0) = 1 - i_0, \quad i(0) = i_0, \quad r(0) = 0. \quad (3)$$

The system (2a-2b) has the drawback that any pair of constants (s_0, i_0) satisfies them, apparently indicating that any pair of values are equilibria. The origin of this problem lies in the fact that (2a-2b) together with (3) do not constitute a well-posed differential problem. Due to the non-locality in time, extended initial conditions must be provided. Mathematically, it is usual to provide arbitrary functions $s(t)$ and $i(t)$ in the interval $[-\tau_0, 0)$. From an epidemiological point of view, however, it is more reasonable to provide just the initial conditions at $t = 0$, and complementary dynamics in the intervals $[0, \tau_i)$: no loss of infectivity or immunity, just local contagion; and $[\tau_i, \tau_0)$: transitions from I to R (the second term of (2a) being absent), and the functions $s(t), i(t)$ already obtained by the initial dynamics.

Indeed, this is the most reasonable choice for the numerical solution of the system, and it is the one we have followed in the numerical results shown below. For the analysis of equilibria, however, an integral representation of the system results into a better-posed problem and the difficulties for the calculation of the equilibria disappear.

An integral equation equivalent to (2b) is:

$$i(t) = c_1 + \beta \int_{t-\tau_i}^t s(u) i(u) du, \quad (4)$$

the interpretation of which is immediate: the integral sums over all the individuals that got infected since time $t - \tau_i$ up to time t . These are all the infectious at time t , since those infected before have already recovered. The integration constant c_1 is, in principle, arbitrary, but it is easy to see that it must be zero since no other sources of infectious exist beyond those taken into account by the integral term.

Complementing (4) it is convenient to write the equation for $1 - r = s + i$, which cancels out the first terms in (2a-2b):

$$s(t) + i(t) = c_2 - \beta \int_{t-\tau_0}^{t-\tau_i} s(u) i(u) du, \quad (5)$$

where, again, c_2 is an integration constant. In this case we have $c_2 = 1$ since no other sources of R exist.

The system (4,5) can be solved for the equilibria of the dynamics, s^* and i^* . One obtains:

$$s^* = \frac{1}{\beta\tau_i}, \quad i^* = \frac{\beta\tau_i - 1}{\beta\tau_0}, \quad (6)$$

which coincides with the equilibria found numerically by integrating (2a-2b), and also corresponds to the same equilibria that can be found in a constant-rate SIRS model (1a), where the rates of recovery and loss of immunity are $1/\tau_i$ and $1/\tau_r$ respectively.

2.2. SIRS with general distribution of infectious and immunity times

The idea behind the fixed-time delays can be generalized to describe more complex dynamics. Let us start with the infected individuals, which is simpler. Consider a probability distribution function $G(t)$, representing the probability (per unit time) of losing infectivity at time t after having become infected at time 0. Observe that the

fixed-time dynamics is included in this description, when $G(t) = \delta(t - \tau_i)$. $G(t)$ can be used as an integration kernel in a delayed equation for the infectious. Indeed, the individuals that got infected at any time $u < t$ and cease to be infectious at time t are:

$$\beta \int_0^t s(u)i(u) G(t-u)du,$$

so that the differential-delayed equation for $i(t)$ is:

$$\frac{di(t)}{dt} = \beta s(t)i(t) - \beta \int_0^t s(u)i(u) G(t-u)du, \quad (7)$$

analogous to (2b).

A second kernel $H(t)$ must be considered for the loss of immunity process. The differential equation for susceptible can then be written as:

$$\frac{ds(t)}{dt} = -\beta s(t)i(t) + \beta \int_0^t \left[\int_0^v s(u)i(u) G(v-u)du \right] H(t-v)dv, \quad (8)$$

where the second term corresponds to individuals that get infected at earlier times, then loose their infectivity at intermediate times with probability G , and finally recover at time t with probability H .

The difficulty with initial conditions that we faced in the fixed-times system is also found here, and can be solved in the same way. Integral equations for $i(t)$ and $s(t) + i(t)$ result:

$$i(t) = c_1 + \beta \int_0^t s(u)i(u)du - \beta \int_0^t \left[\int_0^v s(u)i(u) G(v-u)du \right] dv, \quad (9)$$

$$s(t) + i(t) = c_2 + \beta \int_0^t \int_0^x \left[\int_0^v s(u)i(u)G(v-u)duH(x-v) - s(v)i(v)G(x-v) \right] dv dx. \quad (10)$$

These equations can be used to find closed expressions for the equilibria which, depending on the functional forms of G and H , can be solved analytically. In general one finds two sets of solutions, the disease free one: $s^* = 1$, $i^* = 0$, and the endemic one bifurcating from it:

$$s^* = \frac{1}{\beta \Sigma_1}, \quad i^* = \frac{\beta \Sigma_1 - 1}{\beta(\Sigma_1 - \Sigma_2)}, \quad (11)$$

with:

$$\Sigma_1 = \int_0^\infty \left[1 - \int_0^v G(v-u)du \right] dv, \quad (12)$$

$$\Sigma_2 = \int_0^\infty \int_0^x \left[H(x-v) \int_0^v G(v-u)du - G(x-v) \right] dv dx. \quad (13)$$

We observe that using either Dirac deltas or exponential functions for the kernels (corresponding to fixed-times and constant rates, respectively), these integrals can be solved analytically to find the equilibria.

Between the two extremes of constant rates and fixed delays, as mentioned, realistic systems are expected to display some extended probabilities distributions for infectious

and immunity times. A convenient interpolation between the exponential and delta distributions that characterize those regimes can be achieved by gamma distributions:

$$G_{p_i}(t) = \frac{p_i^{p_i} t^{p_i-1} e^{-p_i t/\tau_i}}{\tau_i^{p_i} (p_i - 1)!}, \quad (14a)$$

$$H_{p_r}(t) = \frac{p_r^{p_r} t^{p_r-1} e^{-p_r t/\tau_r}}{\tau_r^{p_r} (p_r - 1)!}. \quad (14b)$$

These distributions have mean τ_i and τ_r respectively, for any value of the parameter $p_{i,r}$. Besides, they interpolate between exponential (when $p_{i,r} = 1$) and Dirac delta distributions (when $p_{i,r} \rightarrow \infty$), with smooth bell-shaped functions for intermediate values of $p_{i,r}$. It can be shown that the equilibria (11) are identical to the classical ones (6) for any $p_{i,r}$.

3. Sustained oscillations in SIRS with delays

Standard SIRS systems, without delays (or equivalently, with $G_1(t)$ and $H_1(t)$ as delay kernels) have either nodes or stable spirals as equilibria. That is, oscillations appear in them as transient regimes damped towards the fixed points. SIRS systems with delays, on the other hand, can exhibit sustained oscillations. These appear as a Hopf bifurcation of the spiral points, controlled by the parameters τ_i , τ_r and β . A linear stability analysis of the fixed-times case can exemplify how this happens.

Assuming that the system (2a-2b) is close to equilibrium, one sets $s(t) = s^* + x(t)$, $i(t) = i^* + y(t)$, obtaining in linear approximation a linear delay-differential system for the departures from equilibrium:

$$\dot{x}(t)/\beta = -i^* x(t) - s^* y(t) + i^* x(t - \tau_0) + s^* y(t - \tau_0), \quad (15a)$$

$$\dot{y}(t)/\beta = i^* x(t) + s^* y(t) - i^* x(t - \tau_i) - s^* y(t - \tau_i). \quad (15b)$$

From this system, proposing exponential solutions $x(t) = c_1 e^{\lambda t}$ and $y(t) = c_2 e^{\lambda t}$, a transcendental characteristic equation is obtained:

$$\lambda^2 + \lambda\beta \left[s^* (e^{-\lambda\tau_i} - 1) - i^* (e^{-\lambda\tau_0} - 1) \right] = 0. \quad (16)$$

Equation (16) can be solved numerically for complex λ , obtaining from its real part the bifurcation line from the stable spirals. This line is shown in figure 3 along with the amplitude of oscillations represented by a colour (gray) map. The amplitude is the result of the numerical integration of the full nonlinear system (2a-2b). Figure 3 condenses the bifurcation phenomenon as a function of the key parameters τ_r/τ_i and R_0 . The black region represents the non oscillating endemic solution. It can be seen that the linear analysis, represented by the line, defines almost exactly the transition.

3.1. Distributed delays: the general case

The fact that we have qualitatively different results regarding the nature of the endemic state for a delta or an exponential distribution gives rise to a fundamental question. Is the existence of an oscillatory endemic state particular to the delta distribution? Or is

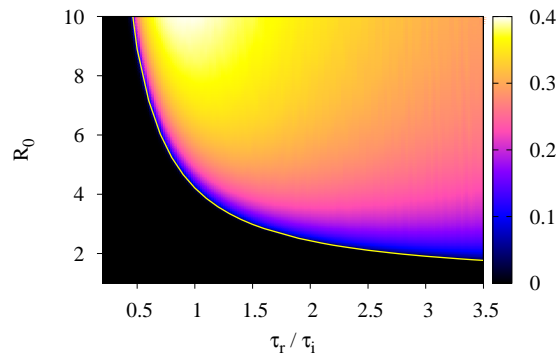


Figure 3. Bifurcation diagram of the SIRS model with fixed times in the space defined by τ_r/τ_i and R_0 . The yellow(white) line shows the linear result. The squared root amplitude of the infectious oscillations is shown as colour (gray) coded shades above the transition line. The black region means zero amplitude, representing non-oscillatory endemic states.

there a critical shape of the distributions G and H necessary for the emergence of the oscillations? Using the Gamma functions defined in (14a) we can check the existence of such solutions for different shapes by controlling the parameter $p_{i,r}$. In this way, we can verify if there is a critical shape $p_{i,r} = p_c(\beta, \tau_i, \tau_r)$ beyond which the system has sustained oscillations at the endemic state. Linearizing the general system (7,8) in the same way presented in the previous section, one has the following integral characteristic equation:

$$\lambda^2 + \lambda\beta i^* \left[1 - \int_0^t \int_0^{t-v} H(v)G(u)e^{-\lambda(u+v)} du dv \right] - \lambda\beta s^* \left[\int_0^t G(u)e^{-\lambda u} du \right] = 0. \quad (17)$$

Using the distributions (14a) in the equation above and taking the limit $t \rightarrow \infty$ we get:

$$\lambda^2 + \lambda\beta i^* \left[1 - \left(1 + \frac{\lambda\tau_i}{p_i} \right)^{-p_i} \left(1 + \frac{\lambda\tau_r}{p_r} \right)^{-p_r} \right] - \lambda\beta s^* \left[1 - \left(1 + \frac{\lambda\tau_i}{p_i} \right)^{-p_i} \right] = 0. \quad (18)$$

As expected, for $p_{i,r} = 1$ and $p_{i,r} \rightarrow \infty$ we recover the characteristic equations of the constant rates and fixed delays models, respectively. Solving (18) numerically for complex λ , one finds that for every set of parameters (provided that $R_0 = \beta\tau_i > 1$) where $p_r > 1$ there is always a critical shape $p_i = p_c$ above which the endemic state consists of sustained oscillations. Conversely, any value of $p_r > 1$ can present sustained oscillations in some region of parameter space. Instead, the constant rate model $p_r = 1$ is a particular case where there is no such solution for any set of parameters, as was demonstrated by Hethcote *et al* ([10]).

Figure 4 shows the real part of the solution of (18) as a function of the shape ($p_{i,r} = p$) of the two time distributions, and for fixed values of the parameters β , τ_i and τ_r . In other words we can appreciate (for those β , τ_i , τ_r) the critical p value (p_c) to have oscillations in the SIRS dynamics, i.e. the value at which $Re[\lambda] = 0$.

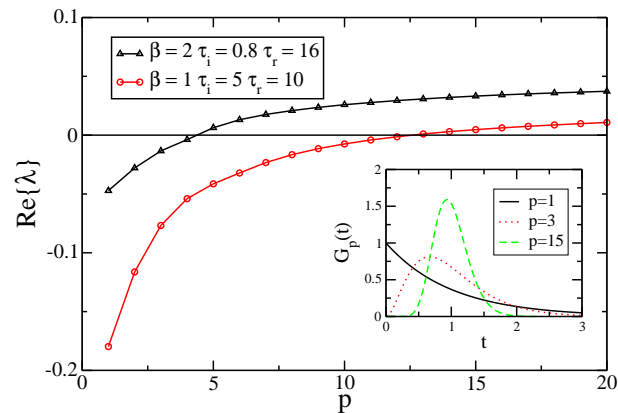


Figure 4. Real part of the eigenvalue λ as a function of the shape parameter $p_r = p_i = p$. Inset: examples of the distribution G_p with $\tau_i = 1$.

The critical shape p_c obtained by numerical calculation of (18) gives an accurate prediction of the emergence of oscillations in the full nonlinear system (7,8), as can be seen in figure 5. The meaning of the critical shape is simple: the time distributions have to be narrower than the one represented by p_c in order to have sustained oscillations.

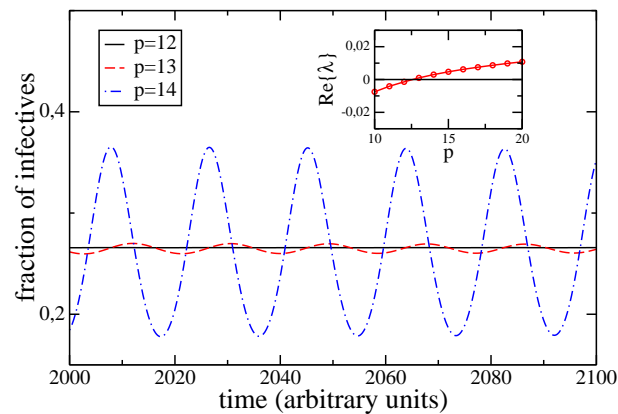


Figure 5. Numerical integration of the SIRS general model with $\beta = 1$, $\tau_i = 5$, $\tau_r = 10$ near the critical shape $p_{i,r} = p_c$ predicted by the linear analysis of the system (inset, $12 < p_c < 13$).

The distributions of infectious and immunity times used so far share a common shape given by the value of p —that made the analysis, restricted to only one shape parameter, simpler. In real situations, though, it is reasonable to expect that these uncorrelated kernels have different shapes, not necessarily of the same relative width. We explore this more general scenario, presenting an oscillation diagram in terms of p_i and p_r in figure 6, for two sets of the SIRS parameters. Some interesting conclusion can be extracted from such diagram:

- If the immunity time distribution is not sharp ($p_r < 5$ for the parameters used in figure 6) there is no oscillation independent of the type of infection time distribution.

- For a relatively narrow distribution of immunity times there is a critical infective time width above which (i.e. a critical p_i below which) no oscillations are obtained.
- The broader one of the time distribution is, the narrower the other one has to be in order to have oscillations.
- Longer immunity times (in units of infectious time) makes the oscillatory region wider in the p_i, p_r space.

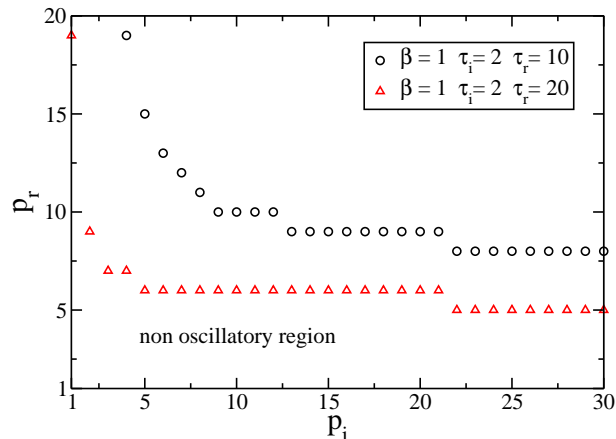


Figure 6. Oscillation diagram in the p_i, p_r plane for two sets of parameters: $\beta = 1$, $\tau_i = 2$, $\tau_r = 10$ (circles) and $\beta = 1$, $\tau_i = 2$, $\tau_r = 20$ (triangles).

In the case $p_{i,r} \rightarrow \infty$ there is a critical value of $R_0(\tau_r/\tau_i)$ above which the endemic solution is always a stable cycle. The linear analysis also shows that for finite $p_{i,r}$ the bifurcation is more involved. Figure 7 shows that the bifurcation line *encloses* a region of oscillating solutions. Then, for a given value of τ_r/τ_i , there is a second critical R_0 , larger than the previous one, where the endemic solution ceases to be cyclic. This phenomenon is verified in the numerical solution of the nonlinear system. For any given τ_r/τ_i , if one increases p the region of oscillation grows (as shown in figure 7), so that in the limit $p_{i,r} \rightarrow \infty$ the upper critical R_0 disappears. In such a situation, the only way to break the oscillations is by decreasing R_0 . On the other hand, by decreasing $p_{i,r}$ the oscillatory region shrinks, disappearing completely when $p_{i,r} = 1$ (exponential distributions, constant rates).

Yet, the interplay between the uncorrelated shapes p_i and p_r and the SIRS parameters is very interesting. Again, in figure 7 we see for example that when $p_i = p_r = 5$ (equal very broad shapes) the oscillation region is very small. But increasing p_i to 20 (narrow infective times distribution), keeping the other fixed, expands the region considerably. Similarly, but in other part of the same diagram, when $p_i = p_r = 20$ (equal very narrow shapes), the region of sustained oscillations is relatively large. Now, by letting the distribution of infective times to be broader ($p_i = 5$) again with the other distribution fixed, we see the oscillatory region to shrink significantly. So, while it is true that the immunity times distribution must be necessarily different from an exponential in order to have oscillations, in general both distributions are relevant to

define the actual parameter region of oscillations. The narrower one or the two are, the wider the oscillatory region is.

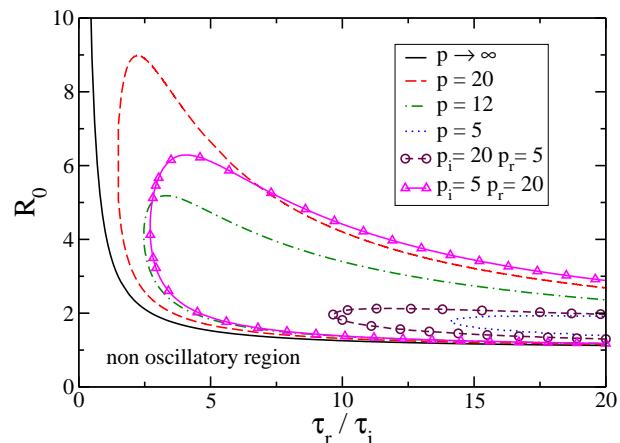


Figure 7. Oscillation diagram in the τ_r/τ_i , R_0 plane for the SIRS model with different distribution for infectious and immunity times controlled by the $p_{i,r}$ -shape factor of the Gamma distribution function. For each pair, p_i , p_r the oscillatory region is enclosed by the corresponding line. The curves with only one p are for $p_i = p_r = p$.

Three examples of dynamics of the SIRS with different shapes sets are displayed in figure 8. The curves correspond to the numerical solution of systems with the same epidemic parameters but three different shape sets: $(p_i = p_r = \infty)$, $(p_i = 1, p_r = \infty)$, and $(p_i = \infty, p_r = 1)$. The first two show the sustained oscillations because the SIRS parameters are inside the oscillatory region, while in the last case we know that there is no possible region of oscillation so we have the damped behavior. Besides, we see that enlarging the τ_i distribution alone, while it shortens the period of the oscillation, it does not destabilizes the oscillation. Remarkably it shows an enhancement of the number of infected during the low part of the cycles. This behavior diminishes the probability of extinction in a discrete population realization of the system, a problem that is common in simulations as we will see in the next section.

From the imaginary part of (18) it is possible to obtain the period of oscillations in the linear approximation. In figure 9 we show the result of this calculation for different shapes of the distributions of infectious and immunity times. For finite $p_{i,r}$, the period of oscillation has a dependency on the parameters that approaches the one found for $p_{i,r} \rightarrow \infty$ (delta distributions, fixed times) in the lower critical value of R_0 , given by

$$T = 3/4\tau_i + 2\tau_r. \quad (19)$$

For a fixed value of τ_r/τ_i , this period decreases as R_0 increases up to the upper limit of oscillation, being bounded from below by $3/4\tau_i + \tau_r$, as shown in figure 9. There are no oscillations above and below these two straight lines, for any value of $p_{i,r}$. This remarkable lock of the period of disease oscillation is related to the one obtained by Taylor and Carr ([11]) in the case of exponential distributed τ_i studied by them.

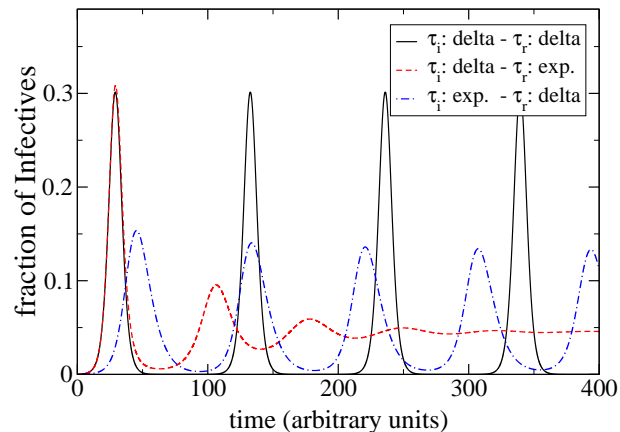


Figure 8. Fraction of infectious as a function of time for three distributions of τ_r and τ_i with different shapes but same parameters $\beta = 0.4$, $\tau_i = 5$, $\tau_r = 50$.

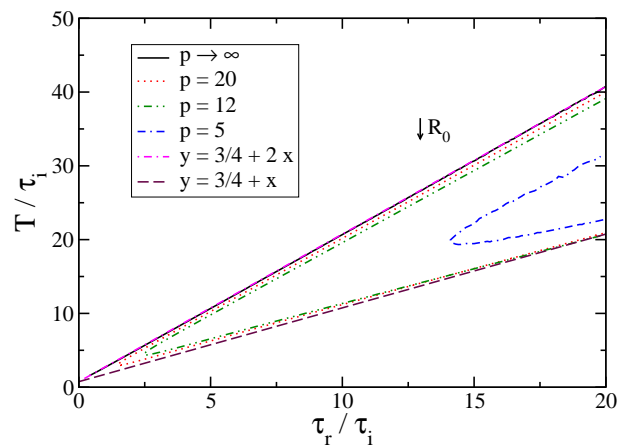


Figure 9. Period of oscillations as a function of τ_r/τ_i . Each curve corresponds to a different shape of the time distributions, as shown in the legend where $p_i = p_r = p$. There are no oscillations above and below the dashed lines.

4. Simulation

A complete picture of the general SIRS dynamics needs to contemplate straightforward numerical simulations. We believe that simulations represent the most accurate implementation of the real system, which is discrete and stochastic. Therefore, as a test of our analytical and numerical results with the generalized SIRS model, we present here results from a probabilistic discrete model. In this model a finite number of agents meet at random and contagion proceeds in a probabilistic way. The phase diagram for such a system, with delta distributions for τ_i and τ_r , is shown in figure 10. The temporal evolution of the system is shown in figure 11 along with the numerical solution of the deterministic model.

The agreement between the two implementations of the same model is very satisfactory, as can be seen by both the bifurcation diagram and the temporal solution. Regarding the diagram the agreement is not as perfect as with the numerical solution

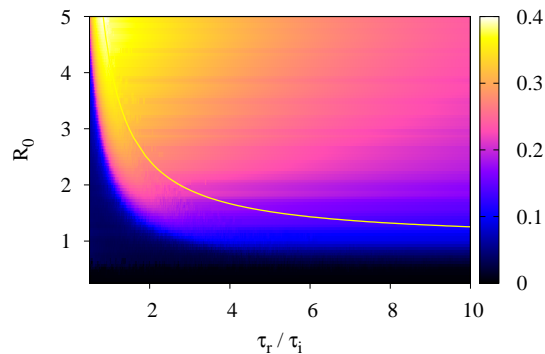


Figure 10. Diagram of the oscillation amplitude, in the τ_r/τ_i , R_0 plane, obtained by simulation with $N = 1000$ agents in the SIRS model with fixed times. Vertical axis is $R_0 = \beta\tau_i$, horizontal axis is the ratio τ_r/τ_i , and the colour (gray) map represent the squared root amplitude of the $i(t)$ at the steady state. The black region means zero amplitude, representing non-oscillatory endemic or non-epidemic states. Superimposed is the critical line obtained by the linear analysis as in figure 3.

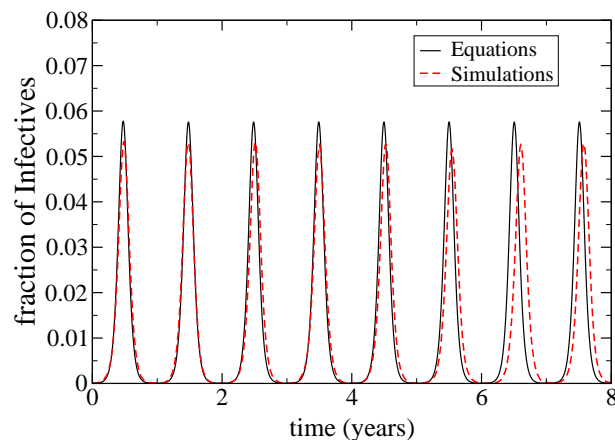


Figure 11. Evolution of an epidemic with stochastic and deterministic models. Time distributions are deltas at $\tau_i = 10days$ and $\tau_r = 180days$, and $\beta = .13perday$. With the time scale in years, the annual oscillation is clearly observed ($T = 2\tau_r + 3/4\tau_i = 367days$).

of the deterministic equations (figure 3) because of fluctuations that arise in simulation due to finite size. These cause large amplitude oscillations which become extinct but that contribute with a non-zero value for the amplitude. As for the temporal evolution, eventually, as time goes by, a small drift develops in the simulation due to the stochastic nature of its dynamics. Far from being disappointing this is a desirable feature, since in real systems epidemic oscillations are not exactly periodic. Yet, the extinctions, that are normally observed in the simulations, are related with the discreteness of them. Long time ago discussed by Bartlett [13] and others it manifests here as being very sensitive to the distance to the lower threshold in the bifurcation diagram, which relates to the

amplitude of the oscillation. Greater amplitudes drive the system closer to the absorbing state at $i = 0$. To illustrate this effect we show in figure 12 three dynamics obtained by simulation with $N = 10^5$ for three different values of β , close to the onset of epidemics and oscillations. However we saw in the previous section (figure 8) that a distribution of infectious times with finite width can increase the lower values of the infectives cycle, which eventually may prevent the extinction in the simulation counterpart.

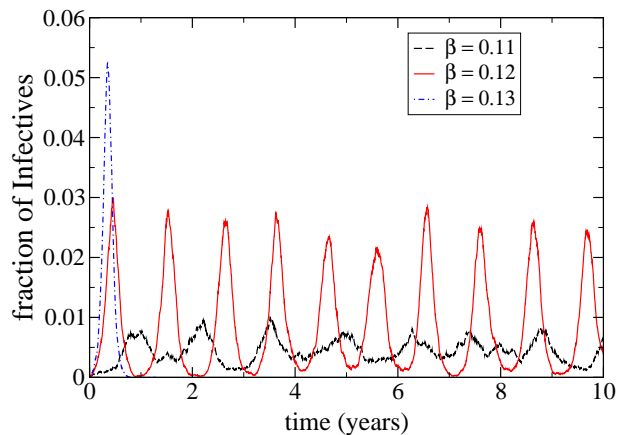


Figure 12. Evolution of the epidemic in the stochastic model, showing extinctions of the infected population. Time distributions are deltas at $\tau_i = 10$ and $\tau_r = 180$ days, $N = 10^5$.

5. Conclusions

We have analyzed a general SIRS epidemic model, in which the infective state as well as the immune state last prescribed times drawn from distributions. These distributed-time transitions constitute a generalization of the standard SIRS model, in which the transitions out of the infective and the immune states happen at a constant rate. The generalization allows for situations in which these states last for certain fixed times—which is more similar to many real diseases than the constant rate assumption. Between the two extremes of constant rates and fixed times, we have also analyzed the intermediate situations of broader or narrower distributions of the transition times.

The generalization runs along the proposals made by previous authors, by implementing the differential equations of the model as non-local in time. For example Hethcote et al. have shown that cyclic models have a transition to oscillatory behavior when the immunity time is distributed [10].

Our contribution shows how the oscillating state arises as a function of all the parameters of the model, completing a phase diagram that provides a thorough and general view of the possible behaviors. We show, moreover, that the linear analysis, the numerical integration of the model, and its stochastic implementation, all converge to the same general picture, within the inherent limitations of each one.

For delta distributed delays (i.e., for fixed times spent in the infective and recovered classes), the phase diagram of figure 3 shows that the region of oscillation is bounded from below by the basic reproductive number R_0 as a function of the scaled immunity time τ_r/τ_i . We see that, as τ_r decreases toward zero, the minimum value of R_0 diverges. This result is in agreement with the fact that in the SIS model there are no sustained oscillations. On the other hand, the amplitude of the oscillations grows both with R_0 and τ_r/τ_i . This kind of behavior may be relevant in the analysis of real epidemics where changes in the parameters are occurring due to interventions, advances in treatment or natural causes. For example, let us imagine an epidemic in the endemic non-oscillating region (shaded black in the diagram), for which, as a desirable consequence of the treatment of the disease, there is an increase in the duration of the immune state, at constant R_0 . As a result, the epidemic may start to oscillate. Such a transition may manifest itself as an initial *increase* of the infectious fraction, due to the onset of oscillation, which should be properly understood in the right context.

We have also shown that the transition to oscillations behaves as a critical phenomenon depending on the *width* of the time distributions. Figure 4 shows this behavior. The remarkable stabilization of the oscillations of pertussis after the introduction of massive vaccination [1, section 6.4.2] may be related to a narrowing of the immunity time distributions.

For distributed delays, corresponding in our model to values of the parameter $1 < p_{i,r} < \infty$, we have found a remarkable reentrance phenomenon in the phase diagram. As exemplified by figure 7, this reentrance means that the region of oscillations is also bounded from above by a curve of R_0 vs τ_r/τ_i . One sees, also, that the region of oscillation shrinks with lowering $p_{i,r}$, until its disappearance at the critical value p_c . Only the case $p_{i,r} \rightarrow \infty$, corresponding to delta distributed times is unbounded. This is at variance with the SIR case analyzed by [14] who claims that there is no significant change between large values of $p_{i,r} = p$ ($p = 10-20$) and $p \rightarrow \infty$. On the other hand our model supports their result in that the region of oscillations is already large for p in this range. An important general result that can be derived from this diagram is the fact that, whenever $\tau_r \gg \tau_i$, the minimum value of R_0 is very close to 1, implying that such systems—provided that $p_{i,r}$ is sufficiently large—are very prone to sustained oscillations. This implies that oscillations due to the implementation of real time distribution into the SIRS formalism are not a marginal or delicate effect as someone could think before.

Our analysis also shows the behavior of the period of oscillation and its dependence on system parameters. Is interesting to discuss this aspect of our model in connection with real infectious diseases. For example in the case of influenza, where the period of oscillation is more or less a year and the infectious time is of the order of 10 days, our model predicts oscillations for any $R_0 > R_{0min} = 1.09$. This minimum value is lower than the usual estimate for this disease, which is around 1.4 [15]. Indeed, this value is so close to $R_0 = 1$ that one can conclude that there will always be oscillations for this disease as long as it remains endemic. Besides we see that using a value of $\tau_r = 180$ days for the loss of immunity, the region of oscillation lays between $1.22 < R_0 < 2.4$

for a rather wide distribution with $p_{i,r} = p = 10$, and $1.16 < R_0 < 3.4$ for a narrower distribution with $p = 30$. In the first case, the corresponding period of oscillation is $188 < T < 342$ (in days), while on the second one it is $190 < T < 360$. Therefore, one needs a narrow distribution to satisfy the observed period of oscillation for influenza. In any case, the predicted region of oscillation includes the observed values of R_0 . We want to stress that, although an infection by a specific strain of the influenza virus confers permanent immunity after the infection period, the mutation rate of the virus can be thought of as an effective immunity period and therefore can also be modeled with the SIRS dynamics.

In the case of other oscillating epidemics, such as syphilis and pertussis, our model also fits the observed data rather well. For syphilis, in the $p_{i,r} \rightarrow \infty$ case, using the period of 132 months measured in United States [3] and the usual value of $\tau_i = 6$ months, we have an $R_{0min} = 1.17$ and $\tau_r \approx 6$ years. Greater values of R_0 (which are expected for syphilis in [3]), with fixed τ_i , predict even longer immune times (which is also the case of syphilis). For pertussis, using the period of 4 years and $\tau_i = 1 - 2$ months, we find $R_{0min} = 1.06 - 1.15$, which is smaller than the estimations obtained for mixing models [15].

In the open field of oscillatory epidemics, we believe that there is a multiplicity of causes that can concur to produce the observed phenomena. Our present contribution does not intend to provide an exclusive and definitive answer to this matter. The construction of valid theoretical models for real diseases should incorporate all the relevant mechanisms, therefore a thorough theoretical investigation of any concurrent possible cause deserves due attention. We hope our work has revealed one good candidate.

Acknowledgments

This work was supported by a cooperative agreement between Brazilian Coordenação de Aperfeiçoamento de Pessoal de Nível Superior and Argentinian Ministerio de Ciencia y Tecnologia agencies (grant CAPES-MINCyT 151/08 - 017/07), and by Brazilian agency Conselho Nacional de Desenvolvimento Científico e Tecnológico (grant CNPq PROSUL-490440/2007). S.G. and M.F.C.G acknowledge financial support from CNPq, Brasil. G.A acknowledges support from Argentinian agencies Agencia Nacional de Promoción Científica y Tecnológica (PICT 04/943), Consejo Nacional de Investigaciones Científicas y Técnicas (PIP 112-200801-00076), and Universidad Nacional de Cuyo (06/C304).

References

- [1] Anderson, R. M. and May, R. M. 1991 *Infectious Diseases of Humans: Dynamics and Control*, Oxford University Press.
- [2] Murray, J. D. 1993 *Mathematical Biology*, Springer.
- [3] Grassly, N. C., Fraser, C. and Garnett, G. P. 2005 *Nature* **433**, 417-421. doi:10.1038/nature03072
- [4] Grenfell, B. and Bjørnstad, O. 2005 *Nature* **433**, 366-367. doi:10.1038/433366a

- [5] Abramson, G. and Kenkre, V. M. 2002 *Phys. Rev. E* **66**, 011912. doi:10.1103/PhysRevE.66.011912
- [6] Risau-Gusmán, S. and Abramson, G. 2007 *Eur. Phys. Jour. B* **60**, 515-520. doi:10.1140/epjb/e2008-00011-7
- [7] Aparicio, J. P. and Solari, H. G. 2001 *Math. Biosciences* **169**, 15. doi:10.1016/S0025-5564(00)00050-X
- [8] Kuperman, M. and Abramson, G. 2001 *Phys. Rev. Lett.* **86**, 2909. doi:10.1103/PhysRevLett.86.2909
- [9] Hoppensteadt, F. C. 1975 *Mathematical Theories of Populations: Demographics, Genetics and Epidemics*. In: *Regional Conference Series on Applied Mathematics*. Philadelphia: SIAM.
- [10] Hethcote, H. W. Stech, H. W. and Van Den Driessche, P. 1981 *SIAM J. Appl. Math.* **40**, 1-9.
- [11] Taylor, M. L. and Carr T. W. 2009 *J. Math. Biol.* **59**, 841-880.
- [12] Gomes, M. F. C. and Gonçalves, S. 2009 *Physica A* **388**, 3133-3142 doi:10.1016/j.physa.2009.04.015
- [13] Bartlett, M. S. 1957 *Journal of the Royal Statistical Society, Series A* **120**, 48-70.
- [14] Black, A. J. McKane, A. J., Nunes, A. and Parisi, A. 2009 *Phys. Rev. E* **80**, 021922-1-9. doi:10.1103/PhysRevE.80.021922
- [15] Hethcote, H. W. 2000 *SIAM Review* **42**, 599-653. doi:10.1137/S0036144500371907